RSC Advances

Synthesis of confined Ru–iongel catalysts and its application for low temperature water–gas shift reaction

SCHOLARONE™
Manuscripts

RSC advance

ARTICLE TYPE

Preparation of confined Ru-iongel catalysts and its application for low temperature water-gas shift reaction

Ting Huang, Bing Liu*, Zehui Zhang, Yuhua Zhang, Jinlin Li*

In this study, a series of iongel catalysts were prepared and studied for the low temperature water-gas shift (WGS) reaction. Compare with the supported ionic liquid (ILs) phase (SILP) catalysts, Ru-iongel catalysts showed better WGS activity and stability. This was mainly due to the strong interaction between ILs and silica support by hydrogen bonding in iongel catalysts. The ILs loading and structure both
10 showed remarkable effect on the catalyst texture, thus affected the catalytic activity. It was found that the activity of iongel catalysts increased with the increase of the ILs loading and the iongel catalysts with the larger anions showed higher catalyst activity over WGS reaction. The iongel catalysts showed certain activity over WGS reaction in the temperature range from 120 ^oC to 200 ^oC, and the highest TOF (66.7 h^{-1}) was obtained at 160 ^oC over 2%Ru30%[BDMIM]BF$_4$@SiO$_2$ catalyst. Through the control experiments
15 and FT-IR technology, ruthenium carbonyl complex was detected to be the active component.

1. Introduction

Currently, the production of high purity hydrogen from fossil fuels has recently attracted considerable attention in chemical industry. Toward this goal, the WGS reaction
20 (CO+H$_2$O→H$_2$+CO$_2$，ΔH=-41.2KJ/mol) is considered to be one of the key steps for the high purity H$_2$ production. This step decreases the minimal CO concentration and at the same time increases the H$_2$ concentration, thus resulting in the production of H$_2$-rich gas stream.[1] WGS reaction is mildly exothermic and
25 equilibrium limited. Industrially, the WGS reaction is typically carried out in two stages: high temperature WGS (300-450 ^oC) by the use of Fe-based catalysts (e.g., Fe$_2$O$_3$/Cr$_2$O$_3$) and low temperature WGS (200-270^oC) by the use of Cu-based catalysts (e.g., Cu/ZnO/Al$_2$O$_3$).[2] However, the commercially available
30 catalysts are not suitable for proton-exchange fuel cells system (PEMFCs) because of the CO level export after low temperature

WGS reaction was still up to 0.1-0.3 wt.%, which poisons the platinum electrode of PEMFCs.[3]

Recently, many heterogeneous catalysts have been developed
35 for WGS reactions, which were mainly focused on the supported noble metal catalysts such as gold, platinum or rhodium on oxide materials.[4-7] As WGS reaction is exothermic and reversible, the low reaction temperature was required in order to get high equilibrium conversion.[3] However, the activity of the catalyst is
40 usually low at a low reaction temperature. In addition, the use of heterogeneous catalysts for WGS reaction sometimes showed some drawbacks such as such as poor precious metal dispersion, sintering and growing up of active sites during reaction process.[8] Thus, it is strongly required to develop highly active catalysts to
45 promote the WGS reaction efficiently under mild conditions.

It has been known long-standing that homogeneous WGS catalysts can be operated at much lower temperatures, favoring higher equilibrium conversions.[9] Ruthenium based homogeneous catalysts have been attracted much interest all the time due to the
50 low cost. For example, [Ru$_3$(CO)$_{12}$] in trimethylamine/water and pyridine-modified ruthenium systems were developed for WGS reactions.[10] These homogeneous catalyst systems could be operated at much lower temperature in compassion with heterogeneous catalyst systems, thus higher equilibrium
55 conversion could be obtained. However, the developed systems demonstrated some distinct drawbacks such as the requirement of high CO pressure (>10 bar) and low catalytic activity.[11,12] Furthermore, the use of volatile solvents would require additional process steps to obtain pure hydrogen without solvent
60 contamination.

T. Huang, Dr. B. Liu, Dr. Z. H. Zhang, Y. H. Zhang, Prof. J. L. Li,
Department of Chemistry, key Laboratory of Catalysis and Material
Sciences of the State Ethnic Affairs Commission & Ministry of
Education.
South-Central University for Nationalities
MinYuan Road 708, Wuhan, R.P. China
Tel:+8627 67842572 & Fax: +8627 67842572
E-mail: liubing@mail.scuec.edu.cn (B. Liu) &jinlinli@yahoo.cn (J. Li)

Compared with the volatile organic solvents, ILs shows some obvious advantages due to the unique characteristics such as low vapor pressure, low combustibility, and excellent thermal stability. Recently, several supported ILs phase (SILP) catalysts were reported to be active for low temperature WGS reactions, in which the catalytically active components (transition metal complexes) are dissolved in ILs.[13] Due to the low vapor pressure of ILs, these catalysts can be facilely applied in gas phase reactions. Recently, Werner et al.[14] prepared SILP catalysts using porous silica to support homogeneous RuCl₃-ILs for WGS reaction under ambient pressure and low temperature. The high catalytic activity of SILP catalysts should be attributed to the following two aspects. Firstly, the active component was homogeneous distribution in ILs medium. In addition, the hydrophilic ILs increased the concentration of water adsorbed on active sites and reduced the adsorption strength of CO at low temperature, leading to a better balance of reactants around active sites. Although ILs show low vapor pressure, SILP catalysts still suffered the risk of leaching of ILs and active component for a long period. For instance, Werner et al., found that a significant deactivation of SILP catalyst was observed after 20 h at 160°C.[15] Therefore, it is still of great interest to develop highly active, selective, cost effective and thermally stable catalysts for low temperature WGS reaction.

The iongel material based catalysts can overcome the above mentioned drawbacks of the SILP catalysts, in which the active components dissolved in ILs were physically confined in solid matrix with desired pore sizes or cavities and channels.[16-18] The solid matrix acts as a nano-scale reactor, and it has large enough pore size for the free transportation of reactants and products. However, the homogeneous metal complex- ILs were confined in the solid matrix.[19] For example, Liu et al prepared a novel iongel catalyst by sol-gel method, in which CuCl₂ dissolved in TEMPO task-specific ILs were confined in a silica-gel matrix. The iongel catalysts showed high catalytic activity and good reusability for aerobic oxidation of alcohols.[20]

Taking the advantages of the high catalytic activity of transition metal complex in ILs and the confinement of iongel materials into consideration, herein, a series of iongel catalysts were prepared and studied for low temperature WGS reaction. To the best of our knowledge, this is the first report that used the iongel catalysts for the low temperature WGS reaction.

2. Experimental Section

2.1 Preparation of iongel catalysts

Procedures for the preparation of the iongel catalysts are shown in Scheme 1. Due to the acidity of the hydrogen connected C2 in imidazolium cation, it can be deprotonated under the alkaline condition to form carbene complex, which was then coordinated with the Ru-carbene complex.[21] In order to exclude the formation of Ru-carbene complex, three kinds of ILs, in which the cations and anions were 1-butyl-2,3-dimethylimidazolium and Cl⁻, BF_4^- or trifluoromethane-sulfonate (OTf⁻), respectively, were employed for the synthesis of iongel catalysts, in which the C-2 was connected with methyl group. Thus they cannot form carbine under the alkaline condition.

Typically, a mixture of tetraethoxyorthosilicate (TEOS, 12-16 mL) and EtOH (20 mL) was heated to 60°C and then ILs (0.5-1.5 g) containing [Ru(NO)(NO₃)₃] (1.0g, containing 9.02 wt.% Ru) were immediately transferred into the TEOS solution. After the formation of a clear and homogeneous mixture, hydrochloric acid (5M, 5 mL) was added and the mixture gradually coagulated. After aging at 60°C for 12 h, the resultant solid material was dried in vacuum at 150°C for 3 h to obtain the iongel catalysts. The prepared catalyst was abbreviated as 2%Ru/x%IL@SiO₂.
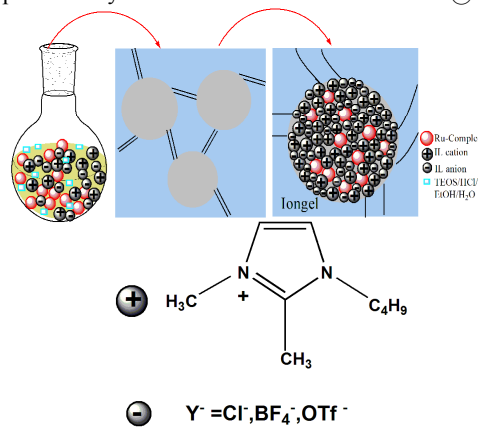
Scheme. 1. Illustration of the synthesis of iongel catalyst.

2.2 Preparation of SILP catalyst

In order to give a comparison with the iongel catalysts, one kind of SILP catalyst was also prepared. The mesocellular foam silica (MCF) with large bimodal pore sizes and 3-D mesostructure was used as the support.[22] Briefly, P123 (12 mg) was firstly dissolved in HCl (2 M, 420 mL), then benzene (24 mL) was added into the solution. Subsequently, tetraethoxyorthosilicate (TEOS, 26mL) was added into the above solution, and the mixture was aged in an oven at 100 °C for 24 h. After that, the white precipitates were filtered, and dried at 120 °C overnight. Finally, the obtained materials were calcined at 550 °C for 6 h to obtain the MCF material. To prepare SILP catalyst, Ru(NO)(NO₃)₃(1.0g, containing 9.06wt.% Ru)and [BDMIM]BF₄ (1.5g) were firstly dissolved in ethanol (20 mL), then the MCF (3.4g) was added into the solution and contiguously stirred for 12 h. The excess solvent was removed through rotary evaporation. The prepared catalyst was defined as 2%Ru/30%[BDMIM]BF₄/MCF.

2.3 Catalysts characterization

BET surface area of the prepared materials was determined by physisorption of N₂ at 77 K by using a quantachrome Autosorb-1-C-MS instrument. The total pore volumes and the average pore sizes were obtained by using the Barrett-Joyner-Halenda method. Prior to measurement, the prepared samples were three times refluxed with acetone at 60°C for 3 times to remove the IL and Ru in the pore and channel.

The X-ray diffraction (XRD) patterns were determined using a Bruker-D8 diffractormeter with monochromatized Cu-Kα radiation (λ = 1.54056 Å) operated at 40 kV and 40 mA and collected by a Vantec-1 detector.

FT-IR measurements were recorded on a Nicolet NEXUS-6700 FTIR spectrometer with a spectral resolution of 4 cm^{-1} in the wave number range of 500-4000 cm^{-1}.

Transmission electron microscopy (TEM) images of the catalyst samples were obtained with a FEI Tecnai G20 instrument. The samples were prepared by directly suspending the catalyst in ethanol with ultrasonic treatment. A copper microscope grid covered with perforated carbon was dipped into the solution and then dried.

Thermogravimetric analysis (TGA) was performed using a PerkinElmer TGS-2 thermal analyzer (Norwalk, CT) with a heating rate of 20℃/min in nitrogen within the temperature range of 40－600℃.

2.4 Typical procedure for WGS reaction

Water-gas shift activities were measured in a continuous test rig with on-line analysis of the effluent gases via Agilent MicroGC 3000A GC. In a typical catalytic experiment, 0.4 g of the as-prepared Ru-iongel catalyst was placed in a stainless-steel tubular fixed bed reactor and contacted with a continuous gas flow (80 ml/min) consisting of 70% N_2, 20% H_2O and 10% CO at 0.3 MPa. The catalyst was first heated in CO/N_2 atmosphere from room temperature to 120°C before steam was added to the mixture. The reaction was firstly conducted at 120°C for about 40 h to keep the catalyst activity stable before the temperature was increased up to 200°C to study the effect of temperature on catalyst activity.

All activities are expressed as CO conversion and turn-over frequency (TOF), defined as below:

$$X_{CO} = ([CO]_{in}-[CO]_{out})/[CO]_{in}$$

$$TOF = V_{CO}\times60\times X_{CO} /22400\times M_{Ru}/m_{Ru} \ (mol_{CO}\,mol_{Ru}^{-1}\,h^{-1})$$

All TOF values were calculated with respect to the total Ru content of the catalyst.

3. Results and Discussion
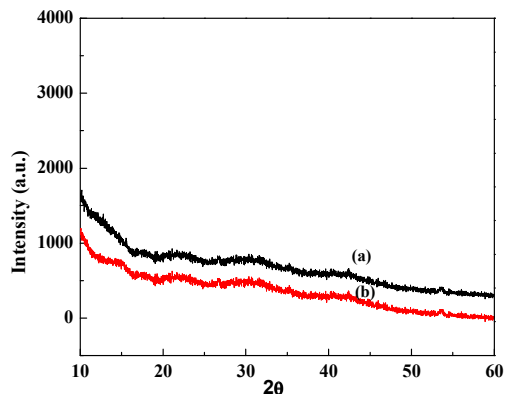
3.1 Characterization of the catalyst

Figure1. XRD patterns of the samples. (a) The silica support obtained by washing the 2%Ru/30%[BDMIM]BF$_4$@SiO$_2$ catalyst; (b) The silica support calcined at 200 ^{o}C.

According to the procedures for the preparation of iongel catalysts, Ru salt dissolved in ILs (Ru-ILs) was confined in the silica matrix. As the Ru-ILs showed no XRD patterns, the silica support was firstly characterized by XRD technology. In order to get the silica support, Ru-ILs was washed off in acetone at reflux temperature for 3 times. As shown in Figure 1, the structure of silica matrix was amorphous. Even though the silica support was calcined at 200°C for 12 h, the XRD pattern was the same. The results indicated that the silica support was stable under our reaction temperature, which was essential to get stable iongel catalysts.
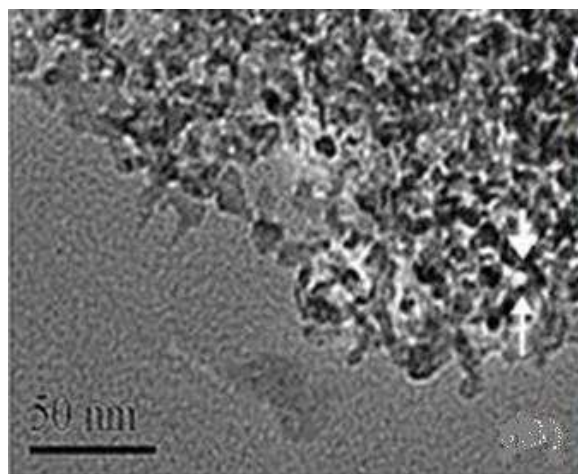

Figure 2. TEM image of silica support

The morphology of the silica support was characterized by TEM image. As shown in Figure 2, it exhibits a disordered wormhole-like pore structure. It is clearly observed that the pores were present in the silica support. As reported in previous results,[23] the presence of ILs during the formation of silica by the hydrolysis of TEOS was responsible for the formation of pores in silica support. Hydrogen bonds between BF_4^- anion and silanol and Π-Π stacking associations between the imidazolium cations played an important role in the directions of pores.[24]

In order to give more insights into the effect of ILs structure and loading on the texture structure of the in-situ formed silica support, BET measurements of various silica supports prepared under different conditions were carried out. Firstly, the effect of the ILs loading on the texture structure of silica supports was studied. Figure 3 displays the N_2 adsorption–desorption isotherms and pore size distribution of the silica support formed in the presence of [BDMIM]BF$_4$ with different loadings (10, 20, 30 wt. %). As shown in Figure 3, all samples show a Type IV isotherm with a large hysteresis, which indicated that all samples presented a 3D intersection network of porous structure.[25] As shown in Table 1, Entries 1, 2 & 3, the ILs loading showed a remarkable effect on the silica surface area and pore size.

The surface area with 20 wt.% ILs was equal to the half of that with 10 wt.% IL. As shown in Table 1, the pore size of the support with 10 wt.% ILs increased greatly from 5.50 to 13.2 nm, while the pore volume increased a little from 1.112 to 1.235 cm^3 g^{-1}. Therefore, under the case of the little difference in the pore

volume between the support with 10 wt.% ILs and the support with 20 wt.% ILs, the increase of pore size with the increase of the weight percent of ILs should result in the decrease of the surface area with the increase of the weight percent of ILs.
[5] However, unlike the change of the texture structure with the weight percentage of ILs from 10 wt.% to 20 wt.%, increasing the ILs loading from 20 wt.% to 30 wt.%, the surface area increased a little compared with 20% ILs loading. This was mainly due to fact that the pore size increased from 13.2 to 16.7 nm, while the
[10] pore volume increased from 1.235 to 1.798 cm^3 g^{-1}. The increasing degree of the pore volume was a little larger than that with the pore size. Therefore, the surface area increased a little from 20 wt.% to 30 wt.%. Our results were consistent with the previous results. [26]

[15] Furthermore, as shown in Figure 3, the pore-size distributions were quite narrow, indicating that the ILs was well confined in the mesoporous silica gel. The effect of the ILs structure on the texture of silica support was also studied, and we paid particular attention on the effect of the anions of ILs. The BET surface of
[20] silica support formed in the presence of [BDMIM]OTf is larger than that in the presence of [BDMIM]BF$_4$, but the pore size and pore volume were less than half of the latter. (Table 1, Entries 1 & 4). The difference in the texture of silica could be better understood from the micro-environment during the formation
[25] process in the presence of different ionic liquids. According to the reports, the strength of the hydrogen bonds between water molecules and OTf$^-$ was stronger than those between water and BF$_4^-$,[27] thus stronger hydrogen bond interactions of OTf$^-$ with silica gel may decrease the interactions between the anion and
[30] imidazolium cation. Additionally, OTf$^-$ is larger than BF$_4^-$, therefore, π–π stackings ofimidazolium rings were blocked and weakened resulting in the relatively disordered arrangement of ILs in the reaction system. Thus, the silica support with smaller pores can be obtained in the presence of [BDMIM]OTf. Our
[35] results were similar with the previous results reported by Zhang et al.,[26] in which they also found the larger surface area and smaller pores of silica matrix were formed in the presence of [BDMIM]OTf in comparison with that in the presence of [BDMIM]BF$_4^-$. From the BET results, it can be clearly seen that
[40] the texture structure of silica gels can be tuned by the variation of IL loading and anion compositions. It can also clearly see in Table 1, the Pore volume of MCF calculated from the BJH model was approximately 1.95 cm^3 g^{-1}, which was similar to 1.798 cm^3 g^{-1} of washed the 2%Ru/30%[BDMIM]BF$_4$@SiO$_2$.
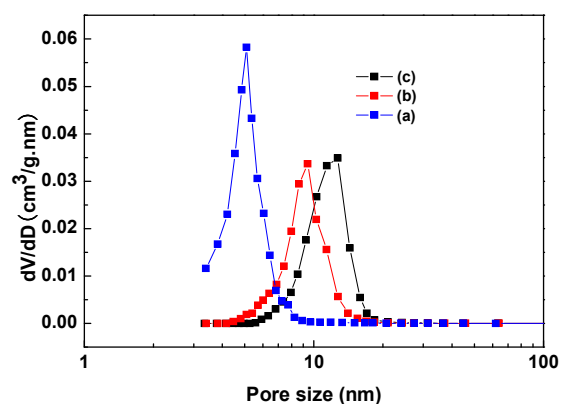

[45]
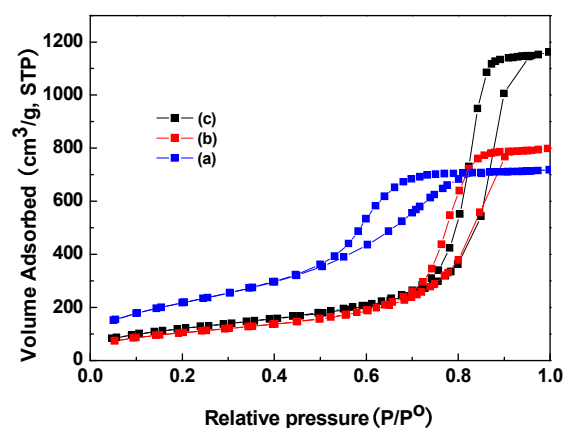
Figure 3. N$_2$ adsorption–desorption isotherms and pore size distribution of washed 2%Ru/x%[BDMIM]BF$_4$@SiO$_2$ with different content, a) 10wt.% IL, b) 20 wt.% IL, c) 30 wt.% IL.

[50] Table 1 Results of N$_2$ adsorption measurements of the silica supports

Entry	ILs	Loading (wt.%)	Surface area (m^2 g^{-1})	Pore diameter (nm)	Pore volume (cm^3 g^{-1})
1	[BDMIM]BF$_4$	10	797	5.50	1.112
2	[BDMIM]BF$_4$	20	374	13.2	1.235
3	[BDMIM]BF$_4$	30	430	16.7	1.798
4	[BDMIM]OTf	10	841	2.03	0.426
5	MCF	30	683.7	Window: 10.1 Cell: 27.6	1.95

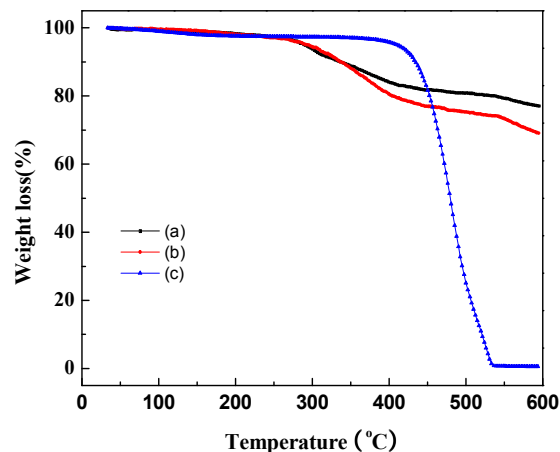Figure 4.TGA of (a) Iongel catalyst: 2%Ru/30%[BDMIM]BF$_4$@SiO$_2$; (b) SILP catalyst: 2%Ru/30%[BDMIM]BF$_4$/MCF catalysts; (c) bulk IL.

The bulk ILs, iongel and SILP catalysts with 30% [BDMIM]BF$_4$ were studied using TGA to understand the role of confinement in the thermal stability of the IL. As shown in Fig. 4, it is clear from the TGA curves that decomposition of the Bulk IL starts at the onset temperature about 384 °C. For SILP and iongel catalyst, the decomposition starts respectively at 289 °C and 291□.In spite of this, the initial decomposition temperature was still higher than those which were used for the water gas shift reaction (below 200°C) in our study. Our TG results were consistent with the previous results reported by Singh et al.[28] They also found the decomposition of IL starts at an earlier temperature upon confinement in nonporous. They proposed a phenomenological 'hinged spring' model to explain this phenomenon, and attributed to the breaking of end group alkyl chains of the ring imidazolium, resulting to an early decomposition temperature.

As shown in Figure 4, there were two main weight-loss regions are found in the two kinds of catalysts. The first step of the decomposition above 400°C could be attributed to the breaking of end group alkyl chains of the [BDMIM]BF$_4$ ring, while the second step (400-600 °C) is likely to be due to the total decomposition of the ILs. [29] In addition, it should point out that Ru(NO)(NO$_3$)$_3$ decomposed together with the decomposition of ILs as it is reported that the decomposition temperature of Ru(NO)(NO$_3$)$_3$ ranged from 180 and 380 °C.[30]Interestingly, it was noted that the weight loss of iongel catalyst was much lower than that of SILP catalyst at the same reaction temperature, indicating that [BDMIM]BF$_4$ confined in silica gel was more stable than that supported on the silica surface. At the final temperature of 600 °C, the weight loss of SILP catalyst was up to 30%, and it was equal to the weight of [BDMIM]BF$_4$, indicating that [BDMIM]BF$_4$ on the surface of silica was completely decomposed. However, the weight loss of iongel catalyst was 23.0%. These data further indicated that [BDMIM]BF$_4$ in iongel catalyst showed higher stability than that in SILP catalyst. The

main possible reason was due to confinement effect. Compared with the SILP catalyst, the ionic liquid and Ru complex confined in the silica gel transferred from the inner pore to external environment less freely than that supported on silica gel (SILP catalyst).
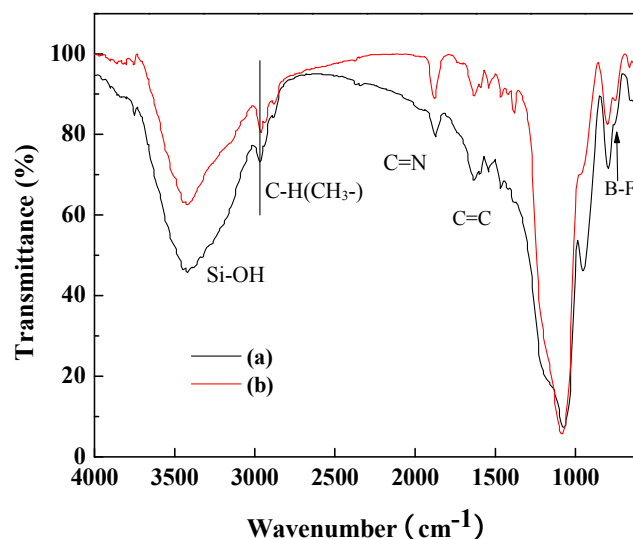

Figure 5. FT-IR spectra of the samples (a) Iongel catalyst: 2%Ru/30%[BDMIM]BF$_4$@SiO$_2$; (b) SILP catalyst: 2%Ru/30%[BDMIM]BF$_4$/MCF catalysts.

Figure 5 shows the FT-IR spectra of the iongel and SILP catalysts, respectively. Three vibration bands at 1540 cm^{-1}, 1875 cm^{-1} and 1630 cm^{-1} are observed for iongel catalyst, which should be assigned to the C=N and C=C vibrations of the imidazole ring. The band at 762 cm^{-1} is the characteristic stretching vibration of BF$_4^{-}$.[31] Two peaks at 749 cm^{-1} and 900 cm^{-1} are assigned to the stretching vibration of C-H in-plane vibration of imidazolium ring.[31] Two bands at 2972 cm^{-1} and 2872 cm^{-1} are due to the C-H stretching of the aliphatic chain connected in the imidazole ring.[32] A strong peak around 1100 cm^{-1} was present in the two catalysts, which was assigned to an asymmetric stretching mode of Si-O-Si. In addition, a broad band around 3450 cm^{-1} was also appeared in the two catalysts, which was attributed to the vibration of surface hydroxyl groups (Si-OH group) or physically adsorbed water.[33] Compared the FT-IR spectra of SILP catalyst with that of iongel catalyst, their FT-IR spectra were almost the same. However, there were still some changes to be noted. It was noted that the C-H vibration bands at 2962 cm^{-1} and stretching vibration of BF$_4^{-}$ at 752 cm^{-1} in the SILP catalyst were shifted to higher wavenumbers at 2972 cm^{-1} and 762 cm^{-1} for iongel catalyst, respectively. These results indicated that the chemical environment of the ILs confined in silica support was different from that of the ILs supported on the silica support and there was some interaction between the ILs and the silica support for the iongel catalyst such as the hydrogen bonding between the BF$_4^{-}$ and the surface hydroxyl groups on the silica support.

3.2 Catalyst WGS activity

3.2.1 Comparison the catalytic activity of our prepared iongel catalysts with SILP catalysts

The catalytic activities of the prepared iongel catalysts were tested for WGS reactions. In order to give an appropriate evaluation of the advantage of our iongel catalysts, WGS reactions over iongel catalysts at low reaction temperatures were firstly compared with the previous reported SILP catalysts, and the results are shown in Table 2. The TOF of the iongel catalysts for WGS reaction at 160 ^{o}C was twice of that for the SILP catalyst at the same reaction temperature (Table 2, Entries 1 *vs* 2). The excellent superiority of the catalytic activity of the iongel catalysts over SILP catalysts was well displayed when WGS reaction was carried out at much lower reaction temperature of 120 ^{o}C (Table 2, Entries 3 & 4). The TOF value for SILP catalyst was only 0.9 h^{-1}, whereas, that was 3.6 h^{-1} for the iongel catalyst. The much more enhancement of the iongel catalysts over SILP catalysts for WGS reaction was consistent with the previous results,[34] albeit they used iongel catalysts for the liquid phase reactions. The TOF of iongel catalysts were higher than those for homogeneous catalyst and SILP catalysts. Therefore, the enhancement of the iongel catalysts was not only due to the homogeneous of the metal complex-ILs in the silica matrix, but also caused by the nanosale confinement effect.

Table 2. Comparison the TOF values of our catalyst with the SILP catalysts with the same Ru precursor and ILs under the same pressure and reaction temperature.

Entry	Catalysts	TOF (h^{-1})$_{max}$	Reaction condition	Reference
1	2%Ru/IL@SiO$_2$ α=10% Ru = RuCl$_3$, IL = [BDMIM]OTf	5.7	P = 0.1 MPa T= 160°C	Our work
2	2%Ru/IL/SiO$_2$ α=10% Ru = RuCl$_3$, IL = [BDMIM]OTf	2.8	P =0.1 MPa, T= 160°C	[14]
3	2%Ru/IL@SiO$_2$α=10% Ru = RuCl$_3$, IL=[BDMIM]OTf	3.6	P = 0.1 MPa T= 120°C	Our work
4	2%Ru/IL/SiO$_2$α=10% Ru = RuCl$_3$, IL = [BDMIM]OTf	0.9	P = 0.1 MPa T = 120°C	[15]

Figure 6 shows the time course of the activity of the iongel catalyst and SILP catalyst. It was found that both the catalytic activity and stability of the iongel catalyst were much better than those of the SILP catalysts. As shown in Figure 6, TOF of the iongel catalyst greatly increased to 20.2 h^{-1} after 2 h, then it rose to 39.3 h^{-1}. It can keep at a stable level of 43 h^{-1} for a long reaction time after a short induction time of 3 h. However, the catalytic activity of SILP catalyst was much lower than that of iongel catalyst, and the TOF around 30 h^{-1}was only obtained after a long induction time of 11 h. More importantly, the SILP catalyst was not as stable as that of the iongel catalyst after a long

reaction time from 26 h to 32 h. Werner et al.,[15]also found that the SILP catalyst was not stable at 160 ^{o}C, in which they believed that the formed active components (Ru-carbonyls) at this temperature stripped from SILP catalyst.
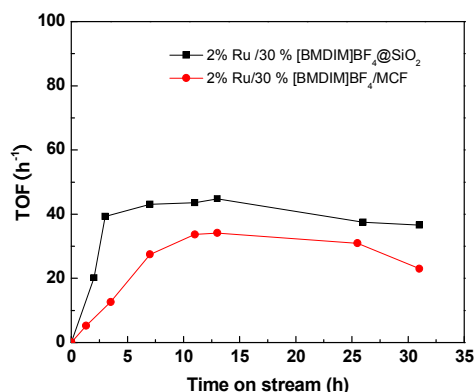

Figure 6. Activity-time profiles of iongel and SILP catalysts. Reaction conditions: T=160°C, P$_{total}$ =0.3 MPa, space velocity of syngas = 12Lg$_{cat}$$^{-1}$ h^{-1}, syngas (10% CO, 20% H$_2$O, N$_2$ balance).

3.2.2 The effect of reaction temperature and ILs loading on the catalytic activity of the iongel catalysts

The effect of the reaction temperature on the activity of iongel catalysts over WGS reactions was also studied and the results are shown in Figure 7. In the study of the effect of reaction temperature on the catalyst activity, the reaction system was firstly subjected to 40 h time-on-stream at 120 ^{o}C, and then the temperature increased to the specific temperature. The reaction was kept at the constant temperature for 6 h, and then the data were collected for specific temperature. Seeing from Figure 7, it was noted that the loading of the ILs in iongel catalysts showed a notable effect on the catalytic activity over WGS reaction at the same reaction temperature. The higher the ILs loading was, the higher the CO conversion was at the same reaction temperature. The following reasons would be helpful to understand the catalyst activity increased with the increase of the ILs loading. On the one hand, as shown in Table 1, the pore size and pore volume of iongel catalysts became gradually larger with the increase of the ILs loading, which reduced the mass transfer resistance for the substrate and product, leading to a higher catalytic activity. On the second hand, much more molecules of CO and H$_2$O would be present around the active sites due to their higher solubility in much more ILs, therefore, the higher catalytic activity was obtained with higher ILs loading.[33]

Furthermore, it was found that the reaction temperature showed a remarkable effect on the catalytic activity of the same kind catalyst. The activity of the catalyst increased sharply from 120 ^{o}C to 160 ^{o}C, and then decreased sharply from 160 ^{o}C to 200°C. The highest TOF was obtained in 67 h^{-1}at 160 ^{o}C with 2%Ru/30%[BDMIM]BF$_4$@SiO$_2$ catalyst. Increasing the reaction temperature from 120 ^{o}C to 160 ^{o}C enhanced the rate coefficient of reaction, thus increasing the catalyst activity with higher CO conversion. However, the catalytic activity decreased beyond 160

^oC, which might be due to that the formed active species were not stable at high temperature.

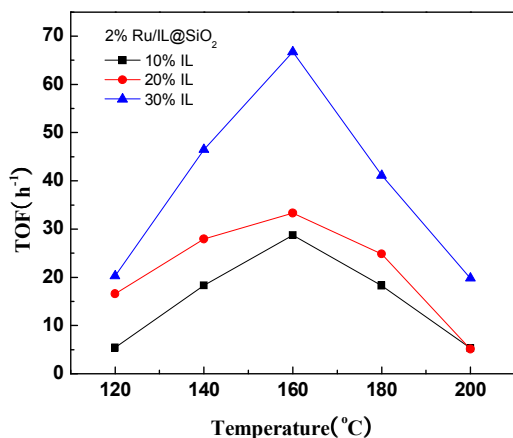Figure 7. The effect of the reaction temperature on WGS activity over 2%Ru/x%[BDMIM]BF$_4$@SiO$_2$ catalysts. Reaction conditions: P$_{total}$ =0.3 MPa, space velocity of syngas = 12 Lg^{-1} h^{-1}, syngas (10% CO, 20% H$_2$O, N$_2$ balance).

3.2.3 The effect of different structure of ILs and Ru complex on the catalytic activity of the iongel catalysts

With the achievement of the optimal reaction temperature and the ILs loading in hand, a series of iongel catalysts with different ILs and different Ru precursor were also studied for WGS reactions. As shown in Table 3, the same cation based ILs with larger anion showed higher catalytic activity than that with smaller anion at the same reaction temperature (Table 3, Entries 1 & 2). As the polarity of [BDMIM]OTf is higher than that of [BDMIM]BF$_4$, much water were be absorbed around active sites. The high concentration of water facilitated the formation of hydroxyl species and effectively enhanced the composition of intermediate species such as formate and carbonate.[33] In addition, it was also reported the solubility of CO was higher in OTf based ILs than that in BF$_4^-$ based ILs.[34] It was reported that ruthenium carbonyl complex was the active component for the homogeneous WGS reaction, which showed high catalytic activity without the requirement of the induction time. Therefore, Ru$_3$(CO)$_{12}$ as the metal precursor was also used to prepare the iongel catalyst, and it was found it indeed showed higher WGS activity at the beginning (Table 3, Entry 3). However, Ru(NO)(NO$_3$)$_3$ based iongelcatalyst required 40 h to incubate its activity (Table 3, Entry 4). In addition, a higher TOF at 120 ^{o}C was obtained from Ru$_3$(CO)$_{12}$ based iongelcatalyst than that obtained from Ru(NO)(NO$_3$)$_3$ based catalyst. Considering the results obtained from Ru$_3$(CO)$_{12}$ and Ru(NO)(NO$_3$)$_3$ based iongelcatalysts, ruthenium carbonyl complexmight be the active component during the long introduction period for Ru(NO)(NO$_3$)$_3$ based catalyst, due to the strong capability of coordination of CO with Ru species.[35]

Table 3. Catalytic results for WGS reaction using a Ru-iongel catalyst system with different ILs.

Entry	Ionic liquid	Precursor	α_{IL} (wt.%)	TOF (h^{-1})$_{max}$	Induction time(h)
1	[BDMIM]BF$_4$	Ru(NO)(NO$_3$)$_3$	10	5.4	43
2	[BDMIM]OTf	Ru(NO)(NO$_3$)$_3$	10	10.5	38
3	[BDMIM]BF$_4$	Ru(NO)(NO$_3$)$_3$	30	7.7	40
4	[BDMIM]BF$_4$	Ru$_3$(CO)$_{12}$	30	11.1	0

Conditions: T=120°C, P$_{total}$ =0.3 MPa, space velocity of syngas = 12 Lg^{-1} h^{-1}, syngas (10% CO, 20% H$_2$O, N$_2$ balance).

3.2.4 Determination of the active species of Ru iongel catalyst

In order to verify the proposed active intermediate, FT-IR technology was used to characterize the fresh Ru(NO)(NO$_3$)$_3$ based iongel catalyst and the used catalyst. As shown in Figure 8, two bands at 2036 and 1890 cm^{-1} were only observed for the used catalyst, which was attributed to the vibration of CO.[34] However, these two bands were not present for the fresh catalyst. These results indicated that ruthenium carbonyl complex was formed during the WGS reaction with Ru(NO)(NO$_3$)$_3$ based iongel catalyst. Our results were similar with the previous results reported by Werner et al.[15] They also observed the formation of dimeric [{Ru(CO)$_3$Cl$_2$}$_2$] when using RuCl$_3$ as the precursor for WGS reaction. The decomposition temperature of Ru$_3$(CO)$_{12}$ was from 160 to 220°C,[36] this also explained why our iongel catalyst gave best WGS activity at 160°C. The formed active species wasn't stable at temperature higher than 160°C, the WGS activity and stability dropped at higher temperature.
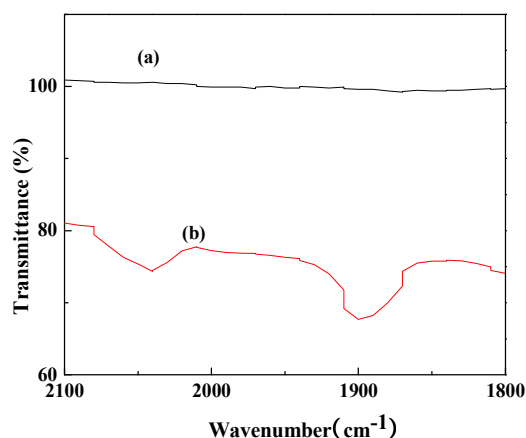

Figure 8. IR spectra of fresh 2%Ru/30%[BDMIM]BF$_4$@SiO$_2$ (a) and the one used in the WGS reaction (b).

4. Conclusion

In conclusion, we have firstly applied the iongel catalysts concept for the low temperature WGS reaction. The best catalytic performance was obtained at a low reaction temperature of 160 ^{o}C. Compared with the reported methods, our developed methods based on iongel catalysts showed some unique advantages, which combined the advantages of the homogeneous and heterogeneous catalysts. On the one hand, the use of the low cost $Ru(NO)(NO_3)_3$ as the metal precursor would be economic for the industrial WGS reactions. On the other hand, the $Ru(NO)(NO_3)_3$ homogeneously dissolved in ILs, and the Ru complex-ILs was quasi-homogeneous. Therefore, the iongel catalyst showed high catalytic activity in a low reaction temperature range from 120 ^{o}C to 160 ^{o}C. In addition, due to the high thermal stability and the confinement of external silica gel, our prepared catalyst also demonstrated a stable TOF (43%) at 160°C and no obvious leaching of the metal at 160°C. Therefore, our method opens a new and highly attractive pathway for the development of the low temperature WGS reaction in the context of future decentralized hydrogen productions.

Reference

[1] N. M. Schweitzer, J. A. Schaidle, O. K. Ezekoye, X. Q. Pan, S. L. Linic, L. T. Thompson, *J. Am. Chem. Soc.*,2011, **133**, 2378.

[2] B. Liu, A. Goldbach, H. Y. Xu, *Catal. Today,* 2011, **171**, 304.

[3] C. M. Kalamaras, I. D. Gonazalez, R. M. Navarro, J. L. G. Fierro, A. M. Efstathiou, *J. Phys. Chem. C.,* 2011, **115**, 11595.

[4] D. Mendes, H. Garcia, V. Silva, A. Mendes, L. Madeira, *Ind. Eng. Chem. Res.*2009, **48**, 430.

[5] B. Liu, T. Huang, Z. H. Zhang, Y. H. Zhang, Z. Wang, J. L. Li, *Catal. Sci. Technol.*, 2014, **4**, 1286.

[6] B. Zugic, D. C. Bell, M. Flytzani-Stephanopoulos,*Appl. Catal. B. Environ.,* 2014, **14**, 243.

[7] T. Barakat, J. C. Rooke, E. Genty, R. Cousin, S.Siffert, B. L. Su, *Energy Environ. Sci.,* 2013, **6**, 371.

[8] R. Kam, J. Scott, R. Amal, C. Selomulya, *Chem. Eng. Sci.*, 2000, **65**, 6461.

[9] P. C. Ford, *Acc. Chem. Res.*, 1981, **14** , 31.

[10] G. Jacobs, B. H. Davis, *Catalysis*, 2007, **20**,122.

[11]S. Werner, N. Szesni, A. Bittermann, M. J. Schneider, P. Härter, M. Haumann, P. Wasserscheid, *Appl. Catal. A: Gen.,* 2010, **377**, 70.

[12] M. Haumann, A. Schönweiz, H. Breitzke, G. Buntkowsky, S. Werner, N. Szesni, *Chem. Eng. Technol.* 2012, **35**, 1421.

[13] R. Knapp, S. A. Wyrzgol, A. Jentys, J. A. Lercher, *J. Catal.,* 2010, **276**, 280.

[14] S. Werner, N. Szesni, R. W. Fishcer, M. Haumann, P. Wasserscheid, *Phys. Chem. Chem. Phys.* 2009,**11**, 10817.

[15] S. Werner, N. Szesni, M. Kaiser, R. W. Fischer,M. Haumann, P. Wasserscheid, *ChemCatChem.,* 2010, **2**, 1399.

[16]Q. Zhang, J. Luo, Y. Y. Wei, *Green Chem.,* 2010, **12**, 2246;

[17] S. Carsten, J. Oriol, E. M. Thomas, S. Stefan, A. L. Johannes, *J. Am. Chem. Soc.,* 2006, **128**, 13990;

[18] Y. L. Gua, G. X. Li, *Adv. Synth. Catal.,* 2009, **351**, 826.

[19] J. Zhang, Q. H. Zhang, X. L. Li, Y. Q. Deng, *Phys. Chem. Chem. Phys.,* 2010, **12**, 1971.

[20] L. Liu, J. J. Ma, J. Y. Xia, L. D. Li, C. L. Li, X. B. Zhang, J. Y. Gong, Z. W. Tong, *Catal. Commun.,* 2011, **12**, 323.

[21] Y. F. Qin, Wei. X, Fang. L, Y. J. Wang, J. F. Wei, *Chin. J. Catal.,* 2011, 32, 1727.

[22] R. Knapp, A. Jentys, J. A. Lercher, *Green Chem.* 2009**, 11**, 656.

[23] P. S.Winkel, W. W. Lukens, P. D. Yang, D. I. Margolese, J. S. Lettow, J. Y. Ying, G. D. Stucky, *Chem. Mater.,* 2000, **12**, 686.

[24] Y. Zhou, J.H. Schattka, M. Antonietti, *Nano Lett.,* 2004, **4**, 477.

[25] F. Shi, Q. H. Zhang, D. M. Li, Y. Q. Deng, *Chem. Eur. J.,* 2005, **11**, 5279.

[26] J. Zhang, Y. B. Maa, F. Shi, L. Q. Liu, Y. Q. Deng, Micropor. Mesopor. Mater., 2009,**119**, 97.

[27] L. Cammarata, S.G. Kazarian, P.A. Salter, T. Welton, *Phys. Chem. Chem. Phys.,*2001, **3**, 5192.

[28] M. P. Singh, R. K. Singh, S. Chandra,J. Phys. D: Appl. Phys., 2010,**43**, 092001.

[29]S. Chen , Y. S. Liu , H. Y. Fu ,Y. X. He , C. Li , W. Huang , Z. Jiang, G. Z. Wu , *J. Phys. Chem. Lett.* 2012, **3**, 1052.

[30]Q. W. Chang, Y. Zhou, C. X, Yan, S. W. Shen, J. zhao, Q. S. Ye, J. Jiang, J. Yu, W. P. Liu, J. L. Chen, *precious metal,* 2013, **34**, 33.

[31] F. Shi, Y. Deng, *Spectrochimica Acta Part A.*, 2005, **62**, 239.

[32] M. P. Singh, R. K. Singh, S. Chandra, *J. Phys. Chem. B.,* 2011,**115**, 7505.

[33] S. J. Craythorne, K. Anderson, F. Lorenzini, C. McCausland, E. F. Smith, P. Licence, A. C. Marr, P. C. Marr, C*hem. Eur. J.,* 2009, **15**, 7094.

[34]C. A. Ohlin, P. J. Dyson, G. Laurenczy, *Chem. Commun.,*2004, **9**, 1070.

[35] A. F. Hill, *Angew. Chem. Int. Ed.*, 2000, **1**, 39.

[36] R. H. Castellanos, E. Borja-Arco, A. Altamirano-Gutiérrez, R. Ortega-Borges, Y. Meas, O. Jiménez-Sandoval, *J. New Mat. Electrochem. Systems,* 2005, **8**, 69.

Acknowledgements